

A novel polyoxometalate-based huge cluster $\text{Fe}_{10}\text{P}_4\text{W}_{32}$ exhibiting prominent electrocatalytic activity for oxygen evolution reaction and third-order NLO properties

Wei Jiang,^{‡, a} Xiao-Mei Liu,^{‡, a} Jian Liu,^b Jie Shi,^a Jia-Peng Cao,^a Xi-Ming Luo,^a and Yan Xu ^{*, a, c}

^a College of Chemical Engineering, State Key Laboratory of Materials-Oriented Chemical Engineering, Nanjing Tech University, Nanjing 210009, P. R. China. E-mail: yanxu@njtech.edu.cn

^b School of Chemistry and Chemical Engineering, Liaoning Normal University, Liaoning 116029, P. R. China.

^c Coordination Chemistry Institute, State Key Laboratory of Coordination Chemistry, Nanjing University, Nanjing 210093, P. R. China

Section 1 Experimental Section	1
I. Materials and General Methods	1
II. Synthesis schemes and method for target compounds.....	1
III. Synthetic discussion.....	2
IV. X-ray Crystallographic Study.....	2
Section 2 Supplementary Structural Information	3
Section 3 Supplementary Physical Characterizations.....	6
Section 4 Additional performance studies	9
I. Electrochemical experiment	9
II. Magnetic measurement	10
III. Electrocatalytic activities experiment.....	11
IV. Nonlinear optical experiment	11
Section 5 The Selected bonds lengths and angles.....	14
References :	19

Section 1 Experimental Section

I. Materials and General Methods

Materials: All the reagents and solvents used for compound synthesis are purchased from commercial sources and used directly without further purification. The $K_{12}[\alpha\text{-H}_2P_2W_{12}O_{48}]\cdot24H_2O$ {P₂W₁₂}, $K_{16}[\alpha\text{-Si}_2W_{18}O_{66}]\cdot25H_2O$ {Si₂W₁₈} precursor and organic ligand DAPSC were prepared by known literature method.¹⁻³

Powder X-ray diffraction (PXRD) patterns were measured on a Bruker D8X diffractometer equipped with monochromatized Cu-K_α radiation ($\lambda = 1.5418 \text{ \AA}$) at room temperature. Data was collected in the range of 5-50 °. Elemental analyses (C, H and N) were determined on a Perkin-Elmer 2400 CHN elemental analyzer. FT-IR spectra were recorded on a Nicolet 8700 FTIR spectrometer with pressed KBr pellets in the range 4000-400 cm⁻¹. EDS test was determined on a Hitachi S-4800. X-ray photoelectron spectroscopy (XPS) was measured on a Thermo ESCALAB 250.

II. Synthesis schemes and method for target compounds

Synthesis of 1: A mixture of $K_{12}[\alpha\text{-H}_2P_2W_{12}O_{48}]\cdot24H_2O$ (0.2 g, 0.0508 mmol), DAPSC (0.02 g, 0.073 mmol), $FeCl_2\cdot4H_2O$ (0.1g, 0.503 mmol) and 10 ml mixed solvent ($H_2O:CH_3CH_2OH = 8:2$) was stirred for 1 h at room temperature. Then adjust the pH = 2.8 with 1M HCl. The resulting mixture was transferred into a Teflon-lined stainless-steel autoclave (25 ml) and heated at 120 °C for 3 days. After the autoclave slow cooled over 12 h at room temperature, the long black strip crystals were harvested, washed with deionized water and then dried at room temperature. Yield: 55 % (based on DAPSC). Elem anal. Calcd (%): C, 4.96; H, 1.48; N, 3.65. Found (%): C, 5.07; H, 1.37; N, 3.76. IR (KBr pellet, cm⁻¹): 3347 (b), 2923 (m), 1660 (s), 1640 (s), 1085 (s), 954 (s), 908 (vs), 772 (s).

Synthesis of 2: $K_{16}[\alpha\text{-Si}_2W_{18}O_{66}]\cdot25H_2O$ (0.2 g, 0.0346 mmol), DAPSC (0.02 g, 0.073 mmol), $FeCl_2\cdot4H_2O$ (0.1g, 0.503 mmol) and Molybdenum powder (0.06 g, 0.625 mmol) were dissolved in 10 ml distilled water and stirred for 1 h at room temperature. Then adjust the pH = 6.0 with 1M NaOH. Then, the mixture was transferred and sealed in a 25 mL Teflon-lined stainless steel container, and heated at 120 °C for 3 days. After the autoclave slow cooled over 12 h at room temperature, the long black strip crystals were obtained, washed with deionized water and then dried at room temperature. Yield: 35 % (based on DAPSC). Elem anal. Calcd (%): C, 7.66; H, 1.91; N, 5.62. Found (%): C, 7.72; H, 2.03; N, 5.73. IR (KBr pellet, cm⁻¹): 3424 (b), 1661 (s), 940 (s), 736 (s).

III. Synthetic discussion

During conventional hydro-/solvothermal method, numerous factors can affect the structures and the crystal growth of the final products. Such as the starting substances (initial reactant, stoichiometric proportion, etc) and the reaction conditions, (pH values, solvents, temperature, reaction temperature, etc). In our works, we obtained two dimer FeSPTs modified by planar Schiff DAPSC complexes $\{\text{Fe}_{10}\text{P}_4\text{W}_{32}\}$ and $\{\text{Fe}_8\text{MoW}_{18}\}$ under solvothermal or hydrothermal condition. Based on our previous works,⁴ POMs-base compounds modified by Schiff base were obtained under the same or similar reaction conditions, which provided us with a lot of useful information to obtain the target product, such as the choice of temperature, solvent and pH value in the reaction system. By choosing appropriate solvent (H_2O , $\text{C}_2\text{H}_5\text{OH}$ DMF, and mixed solvent) and changing the pH of initial reactant, the target compounds can be obtained. In addition, a large number of parallel experiments were also implemented to explore the optimal conditions for reaction synthesis (pH = 2.8, $\text{H}_2\text{O}:\text{C}_2\text{H}_5\text{OH} = 8:2$ mL, $T = 120^\circ\text{C}$, $t = 3\text{d}$ for **1**; pH = 6, $\text{H}_2\text{O} = 10$ mL, $T = 120^\circ\text{C}$, $t = 3\text{d}$ for **2**). During the reaction, both $\{\text{P}_2\text{W}_{12}\}$ and $\{\text{Si}_2\text{W}_{18}\}$ were separated and self-assembled into new $\{\text{P}_2\text{W}_{14}\}$ and $\{\text{MoW}_{18}\}$ BBs. Based on numerous repeated experiments, the synthesized compounds showed good reproducibility and stable yield.

IV. X-ray Crystallographic Study

Single-crystal X-ray diffraction: Single-crystal X-ray diffraction data for **1** and **2** were performed on a Bruker Apex II CCD equipped with a normal focus at 296 K, with a sealed tube X-ray source (Mo-K α radiation, $\lambda = 0.71073$ Å) under the operate condition at 50 kV and 30 mA. The structure were solved by direct methods and refined by full-matrix least-squares refinement using the SHELXL-2018/3 program package. Anisotropic thermal parameters were used to refine all non-hydrogen atoms.

Table S1. Crystal data and structure refinement parameters for compounds **1** and **2**

Compounds	1	2
Formula	$\text{C}_{44}\text{H}_{142}\text{Fe}_{10}\text{N}_{28}\text{Na}_4\text{O}_{169}\text{P}_4\text{W}_{32}$	$\text{C}_{44}\text{H}_{134}\text{Fe}_8\text{MoN}_{28}\text{O}_{113}\text{W}_{18}$
F_w	10425.39	6715.82
T (K)	296(2)	296(2)
Space group	$P\text{-}1$	$P2(1)/n$
$a/\text{\AA}$	14.2296(13)	11.929(2)
$b/\text{\AA}$	15.8958(14)	31.857(7)
$c/\text{\AA}$	23.381(2)	19.576(4)
$\alpha/^\circ$	75.199(10)	90
$\beta/^\circ$	87.381(10)	103.082(3)

$\gamma/^\circ$	68.625(10)	90
$V/\text{\AA}^3$	4754.7(7)	7246(3)
Z	1	2
$D_c (\text{g}\cdot\text{cm}^{-3})$	3.641	3.078
$\mu (\text{mm}^{-1})$	20.166	15.195
$F(000)$	4686	6160
Theta range for date collection	0.902 to 25.01	1.245 to 27.003
Crystal size(mm)	0.14×0.13×0.12	0.12×0.11×0.1
Limiting indices	-16≤ h ≤16 -18≤ k ≤18 -24≤ l ≤27	-14≤ h ≤14 -33≤ k ≤40 -23≤ l ≤24
Completeness	98.6 %	99.9 %
Data/restraints/parameters	16517/684/ 1316	14461/54/ 965
Reflections collected	33456	53336
Independent reflections	16517	14461
R_{int}	0.0500	0.0691
Final R_1^a , wR_2^b [$I > \sigma(I)$]	0.0444, 0.1090	0.0512, 0.1147
Final R_1^a , wR_2^b (all data)	0.0679, 0.1231	0.0752, 0.1257
GOF on F^2	0.990	1.08

^a $R_1 = \Sigma |F_o| - |F_c| / \Sigma |F_o|$; ^b $wR_2 = \{\sum [w(F_o^2 - F_c^2)^2] / \sum [w(F_o^2)^2]\}^{1/2}$

Section 2 Supplementary Structural Information

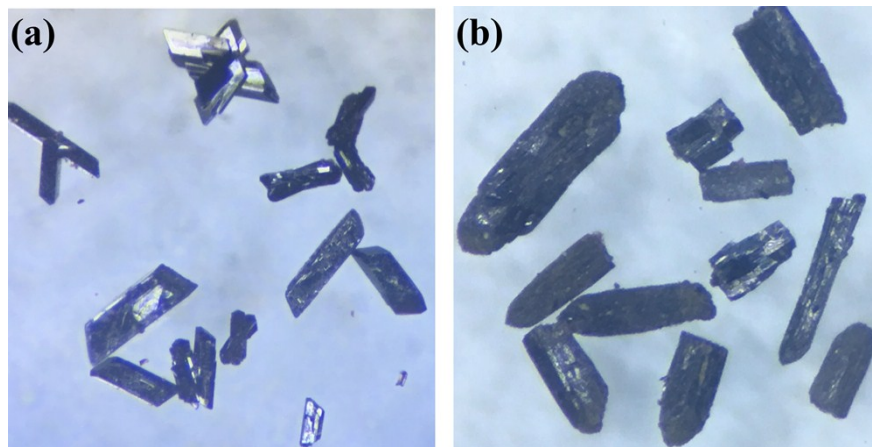


Fig. S1 The photographs of compound **1** (a) and compound **2** (b) under an optical microscope.

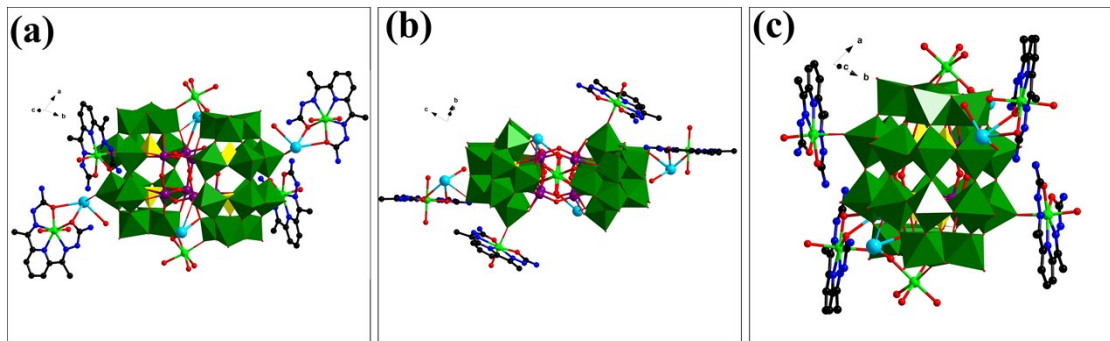


Fig. S2 Polyhedral and ball-and-stick representation of **1** in different orientations: front view (a), right view (b), top view (c). Color code: PO_4 (yellow tetrahedra), WO_6 (green octahedra); W (green); Fe/W (purple); P (yellow); Fe (bright); Na (turquoise); O (red); C (black) and N (blue).

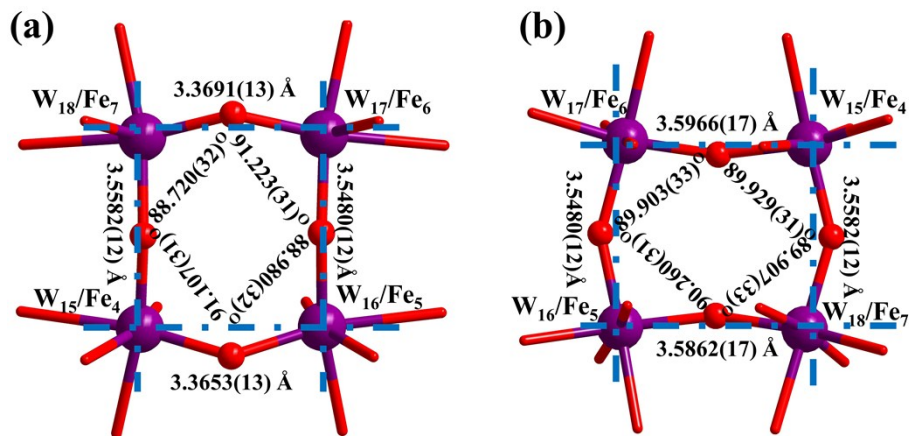


Fig. S3 Connection patterns of $\{\text{Fe}_2\text{W}_2\}$ unit in the quasi-cubane $\{\text{Fe}_4\text{W}_4\}$ core (a) front-view, (b) left-view. Color code: W (green); Fe/W (purple); Fe (bright) and O (red).

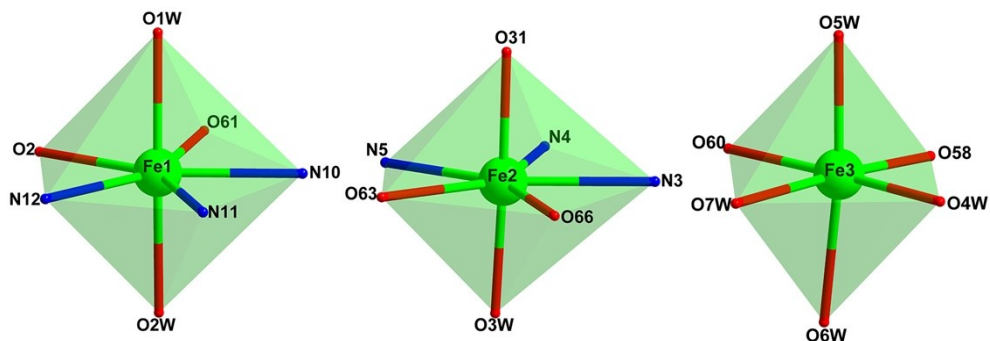


Fig. S4 The coordination modes of iron ions of compound **1**.

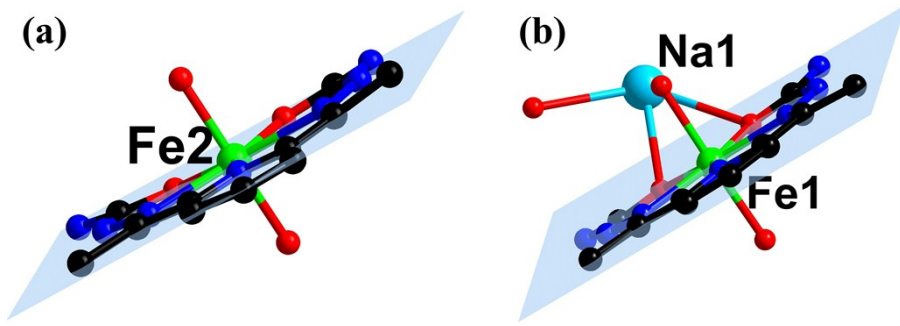


Fig. S5 The rigid planar surface of all the non-hydrogen atoms in $[\text{Fe}^{\text{II}}(\text{H}_2\text{O})(\text{DAPSC})]^{2+}$ (a) and $[\text{Na}(\text{H}_2\text{O})\text{Fe}^{\text{II}}(\text{H}_2\text{O})_2(\text{DAPSC})]^{3+}$ (b) fragments of compound 1.

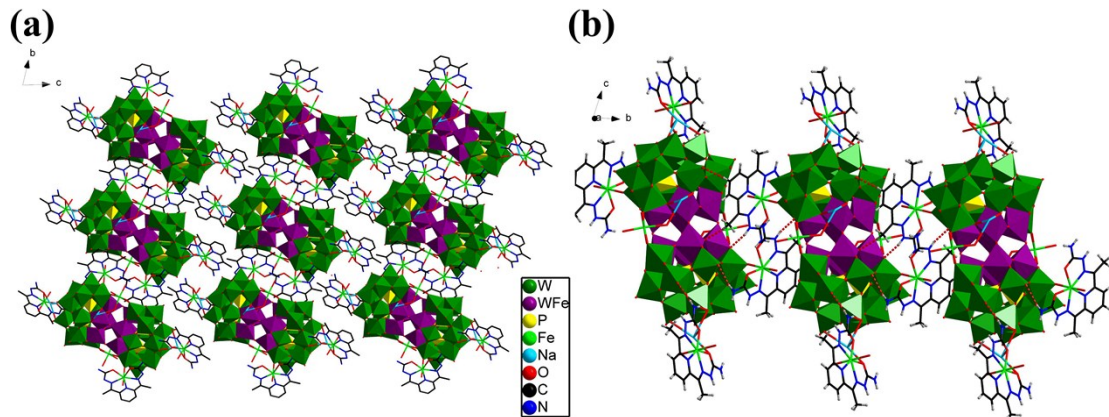


Fig. S6 (a) Polyhedral and stick representation of 3D supramolecular framework of compound 1. (b) The hydrogen-bonding interactions in compound 1.

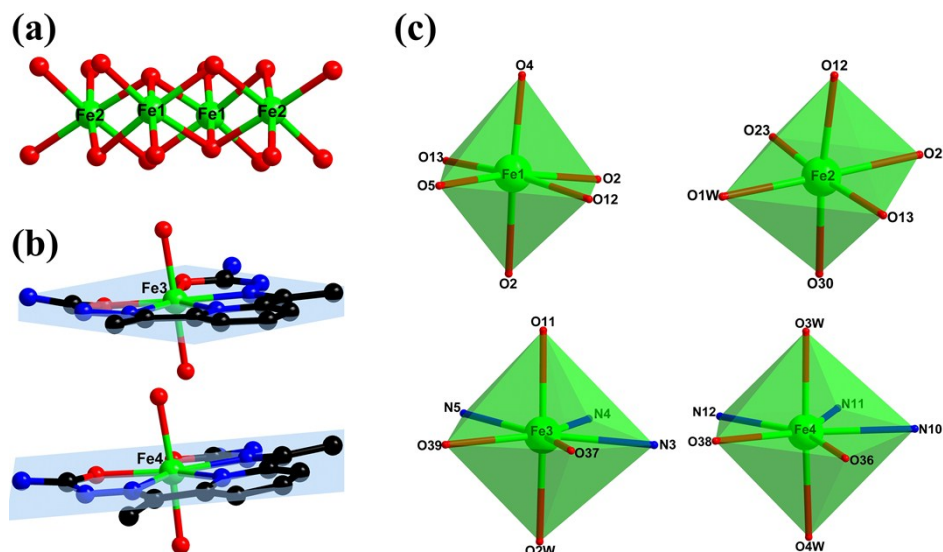


Fig. S7 (a) Connection patterns of $[\text{Fe}^{\text{III}}_4(\text{H}_2\text{O})_2]^{12+}$ metal cluster in 2a. (b) The rigid planar surface of all the non-hydrogen atoms in $[\text{Fe}^{\text{III}}(\text{H}_2\text{O})(\text{DAPSC})]^{3+}$ and $[\text{Fe}^{\text{II}}(\text{H}_2\text{O})_2(\text{DAPSC})]^{2+}$ fragments of 2. (c) The coordination modes of iron ion of compound 2.

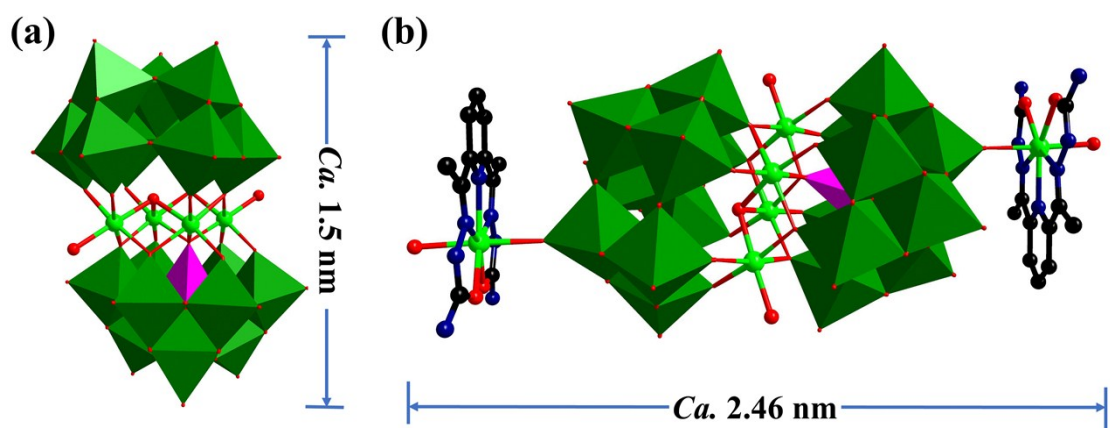


Fig. S8 Polyhedral and ball-and-stick representation of **2a** (a) and **2** unit (b). Color codes: MoO_4 (pink tetrahedra), WO_6 (green octahedra); Mo (pink); W (green); Fe (bright green); O (red); C (black) and N (blue).

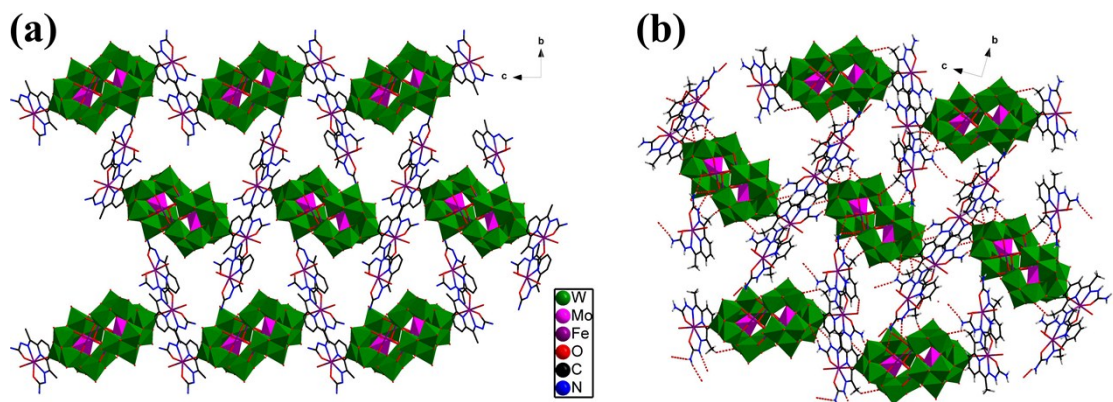


Fig. S9 Polyhedral and stick representation of 3D supramolecular framework of compound **2** (a). The hydrogen-bonding interactions in compound **2** (b).

Section 3 Supplementary Physical Characterizations

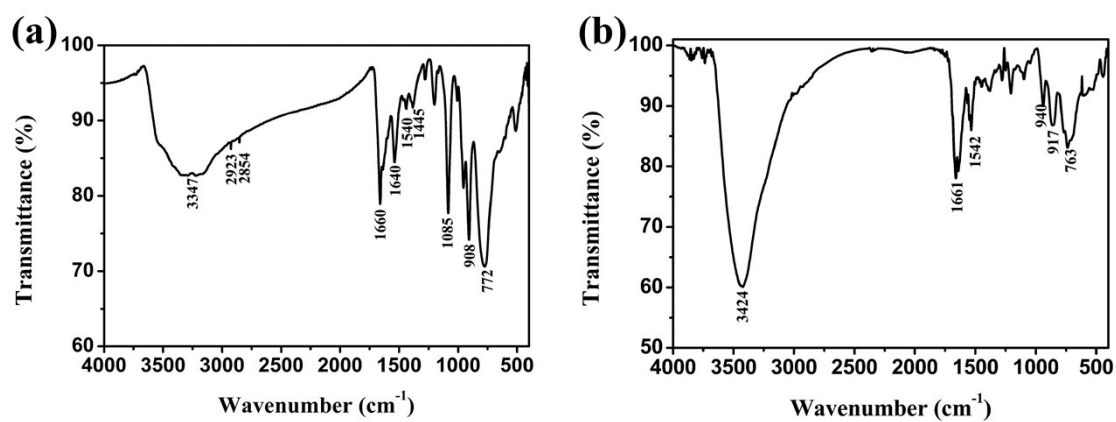


Fig. S10 IR spectra of compound **1** (a) and compound **2** (b).

The IR spectra analysis of the target compound

The IR spectra of the compound **1** and compound **2** were recorded between $\nu = 4000 - 400 \text{ cm}^{-1}$ is shown in Fig. S12. These characteristic peaks can be summarized in two parts as following. DAPSC: 2923 cm^{-1} , 2954 cm^{-1} , 1445 cm^{-1} , 1381 cm^{-1} (**1**) and 2925 cm^{-1} , 2851 cm^{-1} (**2**) for ν (C-H), 1660 cm^{-1} , 1640 cm^{-1} (**1**) and 1661 cm^{-1} 1640 cm^{-1} (**2**) for ν (C=O), 1540 cm^{-1} (**1**) and 1542 cm^{-1} (**2**) for ν (C=N); $[\text{P}_4\text{W}_{32}\text{O}_{120}]^{28-}$ anion: 1085 cm^{-1} for ν (P-O), 954 cm^{-1} for ν (W=O), 908 cm^{-1} and 772 cm^{-1} for ν (W-O-W), $[\text{MoW}_{18}\text{O}_{68}]^{22-}$ anion: 782 cm^{-1} for ν (Mo-O), 940 cm^{-1} for ν (W=O), 917 cm^{-1} for ν (W-O-W), which similar to compounds reported in the literature.⁴ Additionally, the broad around at about 3347 cm^{-1} (**1**) and 3424 cm^{-1} (**2**) indicates the presence of water molecules.

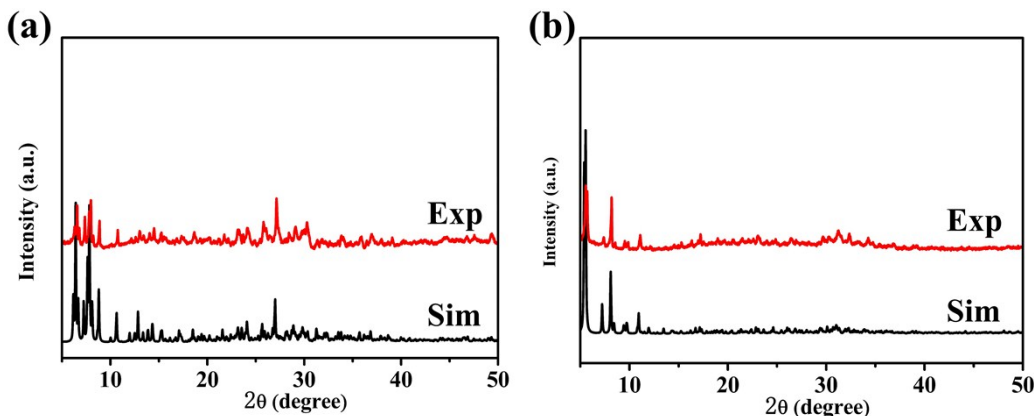


Fig. S11 The experimental and simulated XRD patterns for compound **1** (a) and compound **2** (b). Sim represents the simulated pattern and Exp represents the pattern of as-synthesized sample, respectively.

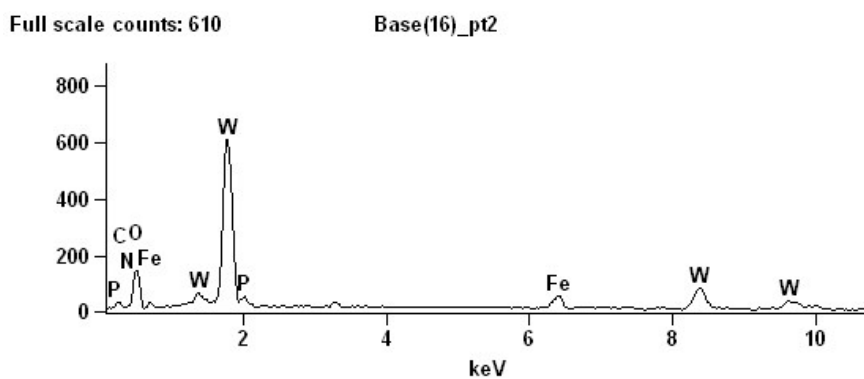


Fig. S12 The EDS images of compound **1**.

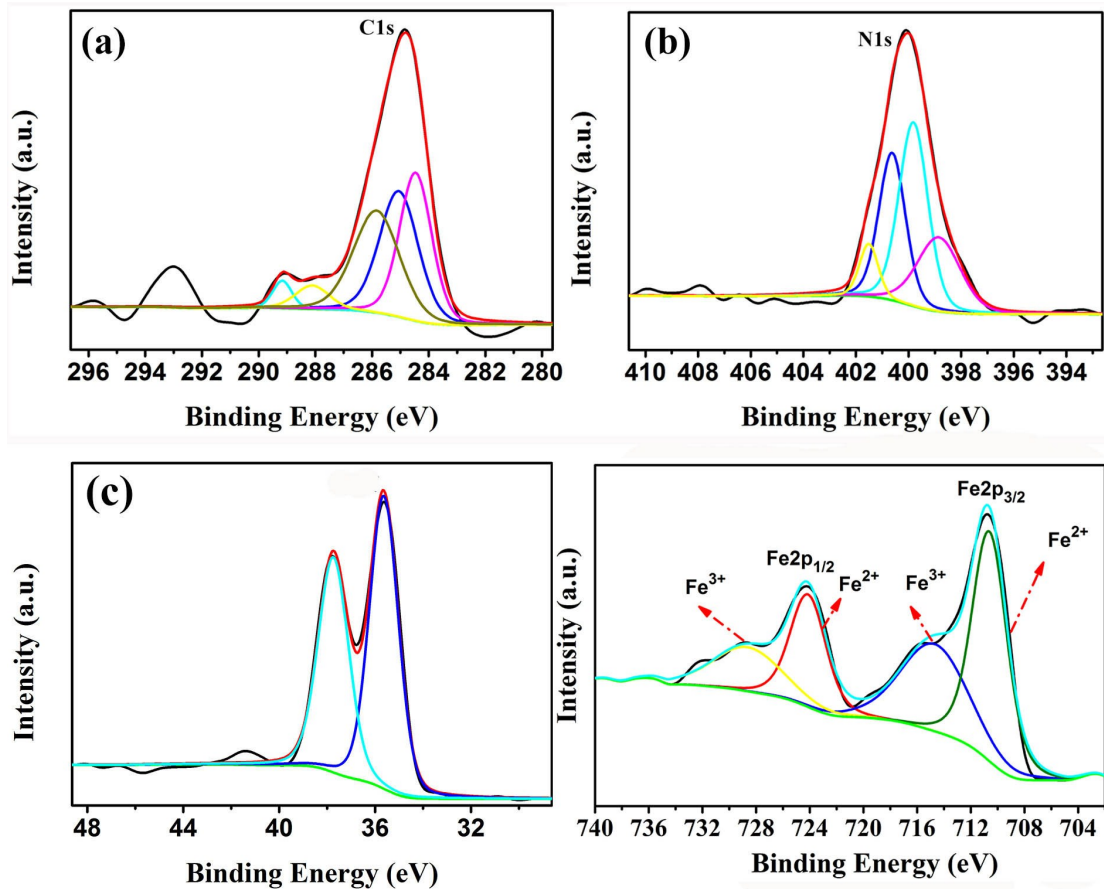


Fig. S13 XPS spectra showing the binding energies of (a) C 1s, (b) N 1s, (c) W 4f and (d) Fe 2p in compound **1**.

XPS spectra analyze:

The C 1s (Fig. S13a) spectra can be divided into five peaks at 284.6, 285.0, 285.8, 288.1 and 290.0 eV ascribed to C atoms in DAPSC ligand (C-H)/(C-C), (C=C), (C-N), (C=N) and (C=O), respectively.⁵ The N 1s (Fig. S13b) spectra can be segmented into four peaks, the peaks at 399.8 ev and the two classic peaks at 400.7 and 401.5 ev can be attributed to amine (-NH₂) group and (C-H) of DAPSC Ligand, and the peaks at 398.8 eV attributed to the interaction of nitrogen bound to the metal (Fe-N).⁶ The W 4f (Fig. S13c) spectra appear two characteristic peaks at 35.6 and 37.8 ev are attributable to W⁶⁺, which accord with the bond valence sum (BVS) calculations.⁷ The Fe 2p (Fig. S13d) spectra appear four classic peaks pick at 728.8, 724.2, 714.9 and 796 ev, which of the peaks at 728.8 and 714.9 ev can indicate the presence of Fe³⁺, other pick at 710.7 and 724.2 ev are attributed to the exist of Fe²⁺.⁸

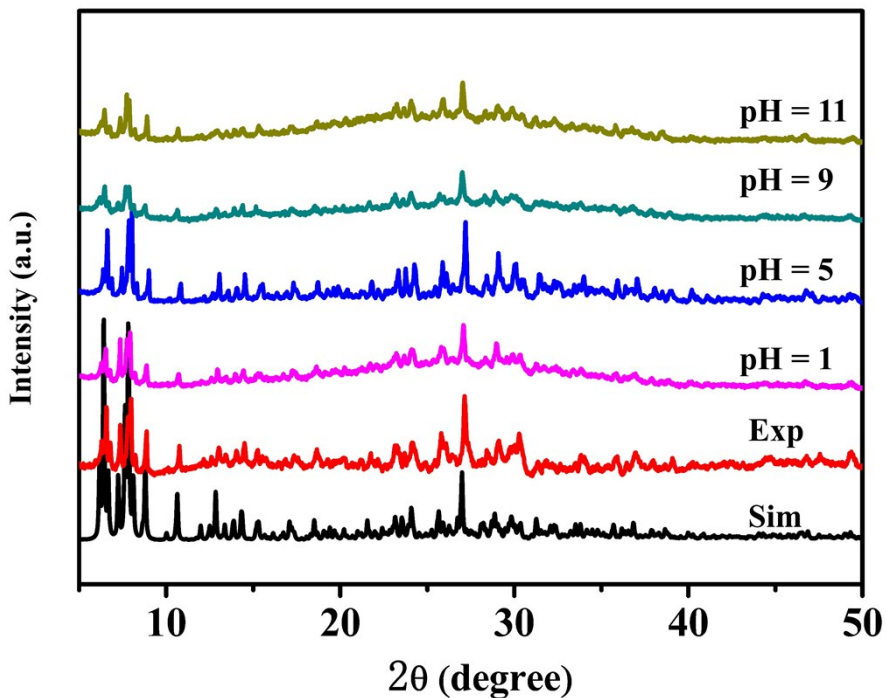


Fig. S14 The PXRD patterns of **1** immersed in water at room temperature for 4 h at different pH. Sim represents the simulated pattern and Exp represents the pattern of as-synthesized sample, respectively.

Section 4 Additional performance studies

I. Electrochemical experiment

Electrochemical measurements were recorded on a CHI760 Electrochemical workstation. A conventional three-electrode cell was used at room temperature. The compound **1** bulk-modified carbon-paste electrode (CPE) was used as the working electrodes. An Ag/AgCl and a platinum wire were used as reference and auxiliary electrodes, respectively.

The electrochemical properties of compound **1** bulk-modified glassy carbon electrode (GCE) were tested in 1 mol L⁻¹ H₂SO₄ aqueous solution at different scanning speeds. As shown in the Fig. S15, **1**-CPE display three pairs of reversible redox peaks in the potential range of -1 to 0.4 V, and the mean peak potentials E_{1/2} = 0.5(E_{pa} + E_{pc}) are -0.552 V (I-I'), -0.262 V (II-II'), 0.122V (III-III') (200 mV s⁻¹), which due to the two-electron redox processes of W centers of {Fe₁₀P₄W₃₂}unit of **1**.⁹ Furthermore, as the scan rate increases (from 100 to 400 mV s⁻¹), the cathodic peak potentials move to the negative direction and the corresponding anodic peak potentials shift to the positive orientation at the same time. In addition, the peak current has a linear relationship with the scanning rate up to 400 mV s⁻¹, which manifest that the redox process of **1**-GCEs is surface-controlled.¹⁰

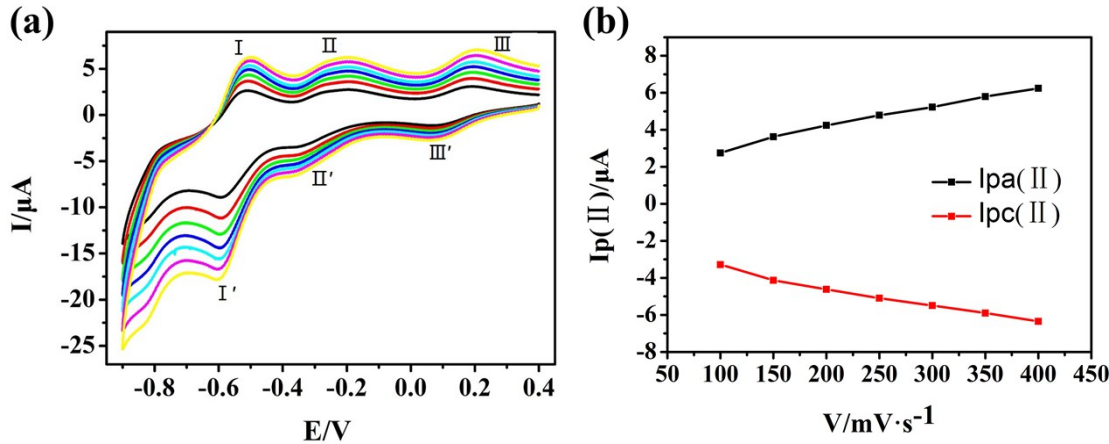


Fig. S15 (a) Cyclic voltammograms of the **1**-CPE in 1 mol L⁻¹ H₂SO₄ aqueous solution at different scanning speeds (from inner to outer: 100, 150, 200, 250, 300, 350, 400 mV s⁻¹). (b) The plots and linear fits of the anodic and the cathodic peaks currents against scan rates for **1**-CPE.

II. Magnetic measurement

The variable magnetic susceptibility data was recorded on a Quantum Design MPMS SQUID magnetometer. The variable-temperature magnetic susceptibilities ($\chi_M T - T$) for complexes **1** were measured from 2–300 K under a constant magnetic field of 1.0 KOe. As shown in the Fig. S16a, at 300K, the $\chi_M T$ value of compound **1** was 37.2 cm³ K mol⁻¹, which is slightly larger than the theoretical value of 35.5 cm³ K mol⁻¹ from four isolated Fe^{III} ions ($S = 5/2$, $g = 2$) and six isolated Fe^{II} ions ($S = 2$, $g = 2$). Upon cooling, the value of $\chi_M T$ decreases slowly and reaches a value of 11.22 cm³ K mol⁻¹ at 2 K. The downward trend of $\chi_M T$ value with decreasing temperature indicates the existence of antiferromagnetic interaction among iron ions in compound **1**.¹¹ As shown in the Fig. S16b, the χ_M^{-1} date of **1** accord with Curie–Weiss law [$\chi_M = C/(T-\theta)$] in the range of 2–300 K. By fitting calculation, we can obtain the Curie constant $C = 37.899$ cm³ and Weiss constant $\theta = -10.251$ K, and the minus Weiss constant further proving the existence of antiferromagnetic interaction in the compound **1**.

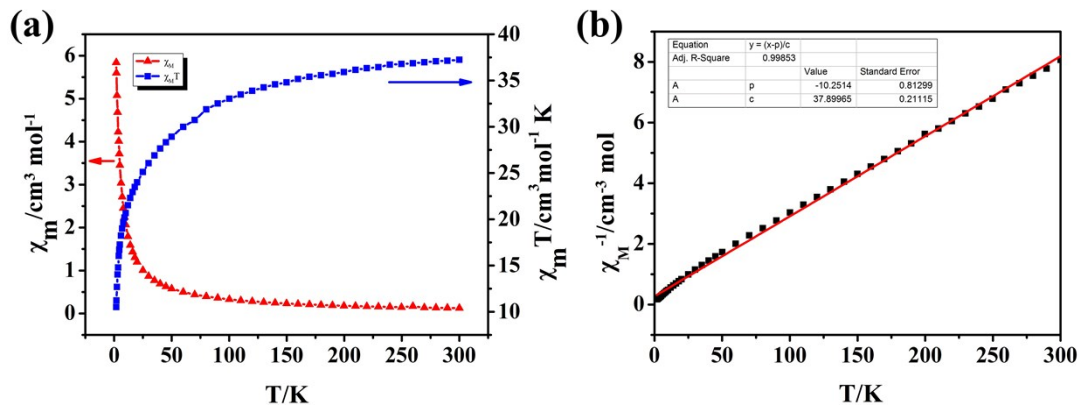


Fig. S16 (a) The χ_M and $\chi_M T$ versus temperature from 2-300 K under 1.0 KOe dc field. (b) The reciprocal magnetic susceptibility χ_M^{-1} versus temperature for compound **1**

III. Electrocatalytic activities experiment

All electrocatalytic measurements were carried out on a ZAHNER IM6ex electrochemical workstation at room temperature under the air atmosphere. In a standard three-electrode cell, the working electrodes were the carbon paste electrode (CPE, 3 mm diameter), a platinum gauze (10 mm × 10 mm) was used as the counter electrode and an Ag/AgCl electrode was the reference electrode. Cyclic voltammetry experiments were carried out in 50 mM Na₂HPO₄ + NaH₂PO₄ buffer (pH = 6.8) with different contents of Fe₁₀P₄W₃₂.

100 mg graphite powder (XC-72) and m g sample Fe₁₀P₄W₃₂ (m = 10 mg, 20 mg and 40 mg, respectively) were mixed according to the mass ratio of 1:0.1, 1:0.2, 1:0.4, and grinded in an agate mortar for 20 minutes, producing a uniform dry mixture. Then 0.1 ml paraffin was added. Finally, the mixture was packed into a glass tube (3 mm diameter) and compacted gently from behind with copper rods, manufacturing CPEs of Fe₁₀P₄W₃₂-C 10%, Fe₁₀P₄W₃₂-C 20% and Fe₁₀P₄W₃₂-C 40%.

Table S2 The different current density versus overpotential of CPEs with different **1** contents.

	Fe ₁₀ P ₄ W ₃₂ (0%)	Fe ₁₀ P ₄ W ₃₂ (10%)	Fe ₁₀ P ₄ W ₃₂ (20%)	Fe ₁₀ P ₄ W ₃₂ (40%)
Current Density (mA cm ⁻²)	Overpotential (mV)			
0.2	262	229	159	118
0.3	330	266	202	160

IV. Nonlinear optical experiment

Two-photon absorption (TPA) cross-sections (σ) were obtained by using Chameleon II femtosecond laser pulse and Ti: 95 sapphire systems.

The electronic spectra of compound **1** and **2** in DMSO solution at a concentration of 1.0×10^{-3} mol L⁻¹ give the nonlinear absorption at room temperature. Two-photon absorption (TPA) values containing TPA coefficient β and TPA cross section σ were measured by the open-aperture Z-scan technique with femtosecond laser pulse and Ti:95 sapphire system. Fig. S17 shows the open aperture Z-scan curves of **1** and **2**. The black dots are the experimental data, and the red lines represent the theoretical simulated curves modified by the following equations (eqn (1) and (2)): ¹²

$$T(z, s=1) = \sum_{m=0}^{\infty} \frac{[-q_0(z)]^m}{(m+1)^{\frac{3}{2}}} \quad \text{for } |q_0| < 1 \quad (1)$$

$$q_0(z) = \frac{\beta I_0 L_{\text{eff}}}{1 + z^2 / z_0^2} \quad (2)$$

where β is the TPA coefficient of the solution, I_0 is the input intensity of laser beam at the focus $z = 0$, $L_{\text{eff}} = (1 - e^{-\alpha L})/\alpha$ is the effective length with α and L are the linear absorption coefficient and the sample length respectively. Z is the sample position, $z_0 = \pi\omega_0^2/\lambda$ is the diffraction length of the beam, in which the ω_0 and λ are the spot size at the focus and the wavelength of the beam respectively. Furthermore, the molecular TPA cross section σ can be calculated by the following relationship:

$$\sigma N_A d \times 10^{-3} = h\nu\beta \quad (3)$$

where N_A , d , h and ν are respectively the Avogadro's constant, the concentration of the compound, the Planck's constant and the frequency of input intensity.

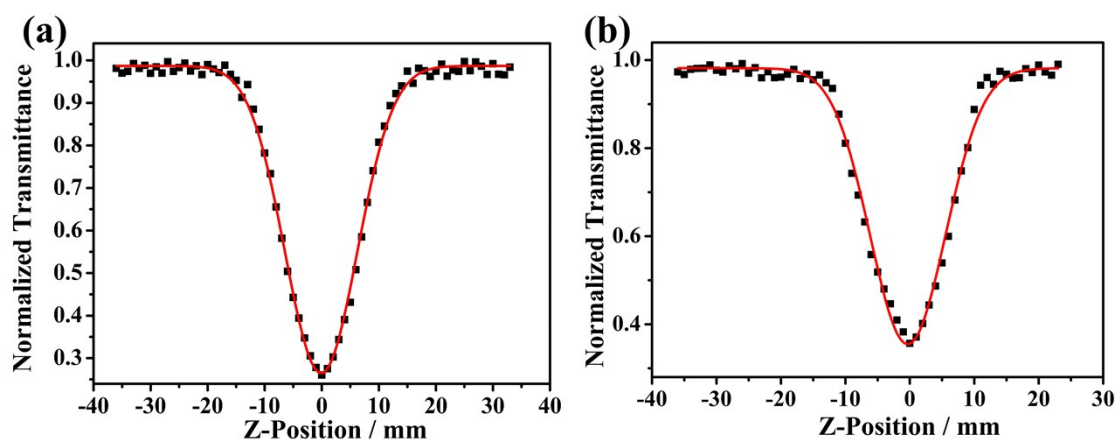


Fig. S17 Z-scan data for compound **1** (a) and compound **2** (b) in DMSO solution at a concentration of 1.0×10^{-3} mol L $^{-1}$ obtained by open aperture Z-scan method.

The particle size of compound **1** in solution was determined by Nano laser particle size analyzer. A mixture of 3.2 mg compound **1** and 3 ml DMF solvent was ultrasonic for 0.5 h to obtain a suspension with a concentration of 1%. Then, the suspension was centrifuged to acquire a supernatant.

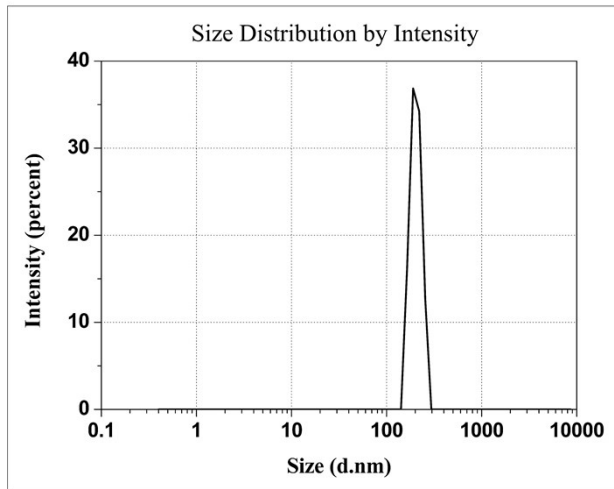


Fig. S18 The particle size of compound **1** in solution

As shown in the figure above, the measured particle size in DMF solvent is about 170 nm, which is much larger than the 3.9 nm. That mainly due to many cluster anions of compound **1** in DMF solvent self-assemble into large particles (a single-layer, hollow spherical "blackberry" structure) with large size. [1]

[1] (a) P. C. Yin, D. Li and T. B. Liu, *Chem. Soc. Rev.*, 2012, **41**, 7368. (b) T. B. Liu, Melissa L. K. Langston, D. Li, J. M. Pigga, C. Pichon, A. M. Todea and A. Müller, *Science*, 2011, **331**, 1590.

Table S3. The third-order NLO data of some POMs-based compound .

Compounds	β^a (cm·GM ⁻¹)	σ^b (GM)	λ (nm)	ref
[Na(H ₂ O)Fe ^{II} (H ₂ O) ₂ (DAPSC)] ₂				
{[Fe ^{II} (H ₂ O)(DAPSC)] ₂ [Fe ^{II} (H ₂ O) ₄] ₂ [Na ₂ Fe ₄ ^{III} P ₄ W ₃₂ O ₁₂₀]•25H ₂ O}	0.04354	2053	700	This work
[Fe ^{II} (H ₂ O) ₂ (DAPSC)] ₂ {[Fe ^{III} (H ₂ O)(DAPSC)] ₂ [Fe ^{III} ₄ (H ₂ O) ₂ MoW ₁₈ O ₆₈]•29H ₂ O}	0.02439	1150	700	
[L-C ₄ O ₆ H ₂) ₂ V ₄ O ₈]•2C ₆ N ₂ H ₁₈	0.003167	1412	740	1
[D-C ₄ O ₆ H ₂) ₂ V ₄ O ₈]•2C ₆ N ₂ H ₁₈	0.003167	1094	740	1
[Co(H ₂ O) ₂ (DAPSC)] ₃ {[Co(H ₂ O)(DAPSC)] ₂ BW ₁₂ O ₄₀ }BW ₁₂ O ₄₀ •10H ₂ O	0.003553	1522	720	2
[Zn(H ₂ O) ₂ (DAPSC)] ₃ {[Zn(H ₂ O)(DAPSC)] ₂ BW ₁₂ O ₄₀ }BW ₁₂ O ₄₀ •8H ₂ O	0.005132	2199	720	2
Na ₂ [(CH ₃) ₂ NH ₂] ₃ {Na \subset [Ce ^{III} (H ₂ O)(CH ₃ CH ₂ OH)(L-tartH ₃)(H ₂ Si ₂ W ₁₉ O ₆₆)]}•3.5H ₂ O	0.01369	389	740	3
[(CH ₃) ₂ NH ₂] ₇ {Na \subset [Ce ^{III} (H ₂ O)(CH ₃ CH ₂ OH)(D-tartH ₃)(Si ₂ W ₁₉ O ₆₆)]}•2.5H ₂ O	0.00279	392	740	3
[Mn(H ₂ O) ₂ (DAPSC)] ₂ {[Na ₃ (H ₂ O) ₂ Mn _{0.5} (H ₂ O) ₄][Mn(H ₂ O)(DAPSC)] ₂ [H ₃ P ₅ W ₃₀ O ₁₁₀]•7.5H ₂ O}	0.002099	888	780	4
[Co(H ₂ O) ₂ (DAPSC)]{[Co(H ₂ O) ₂ (DAPSC)][Na _{1.5} (H ₂ O) ₂]•[Na _{0.5} (H ₂ O) ₂]•2H ₂ O}				

$5(H_2O)_2Co_{0.5}(H_2O)_4][Co(H_2O)(DAPSC)]_2[H_4P_5W_{30}O_{110}] \cdot 6H_2O$	0.001715	707	800	4
$[Ni(NTB)(H_2O)]_2(H_2P_2Mo_5O_{23}) \cdot 9.25H_2O$	0.001655	758	720	5
$[Ni(H_2O)(NTB)]_2(PMo^{VI}_{11}Mo^V O_{40}) \cdot 4.5H_2O$	0.001127	404	920	5
$[Ni(NTB)]_2(Mo_8O_{26}) \cdot 9H_2O$	0.015925	673	780	5
$[Co(H_2O)_6] \{[C_3H_4N_2]_2[C_5NH_5]_{14}[H_{15}(Mo_2O_4)_8Co_{16}(PO_4)_{14}(HPO_3)_{10}(OH)_3]\} \cdot 5H_2O$	0.01375	622	730	6
$[C_3H_5N_2]_4[C_5NH_5]_2[Ni(H_2O)_6] \{[C_3H_4N_2]_2[C_5NH_5]_{14}[H_{18}(Mo_2O_4)_8Ni_{16}(PO_4)_{22}(OH)_6]\} \cdot 11H_2O$	0.0056	274	750	6
$[C_5NH_5]_8[C_3H_5N_2]_2 \{[C_5NH_5]_9[H_{31}Mo_{12}O_{24}Co_{12}(PO_4)_{23}(H_2O)_4]\} \cdot 12H_2O$	0.00263	1058	820	7
$[Sm(H_2O)_2(DAPSC)]_2[Sm(H_2O)_3(DAPSC)]_2[(SiW_{12}O_{40})]_3 \cdot 15H_2O$	0.021047	1383	680	8
$[Eu(H_2O)_2(DAPSC)]_2[Eu(H_2O)_3(DAPSC)]_2[(SiW_{12}O_{40})]_3 \cdot 15H_2O$	0.013874	669	700	8
$[Tb(H_2O)_2(DAPSC)]_2[Tb(H_2O)_3(DAPSC)]_2[(SiW_{12}O_{40})]_3 \cdot 15H_2O$	0.011443	712	720	8

^a TPA absorption coefficient of the solution. ^b molecular TPA cross-section.

Table S4. BVS analysis of compound **1** for iron atom

BVP	S	BVP	S	BVP	S
Fe(1)-O(61)	0.3111	Fe(2)-O(31)	0.3894	Fe(3)-O(4W)	0.4469
Fe(1)-O(2)	0.2876	Fe(2)-O(3W)	0.3769	Fe(3)-O(60)	0.3947
Fe(1)-N(10)	0.3523	Fe(2)-O(66)	0.3533	Fe(3)-O(58)#1	0.3852
Fe(1)-O(1W)	0.2838	Fe(2)-N(4)	0.3679	Fe(3)-O(5W)	0.3401
Fe(1)-N(11)	0.3411	Fe(2)-N(3)	0.3356	Fe(3)-O(7W)	0.2846
Fe(1)-N(12)	0.3329	Fe(2)-N(5)	0.3240	Fe(3)-O(6W)	0.2554
Fe(1)-O(2W)	0.2718	Fe(2)-O(63)	0.2610		
BVS	2.1806		2.4080		2.1069

Table S5. BVS analysis of compound **2** for iron atom

BVP	S	BVP	S	BVP	S	BVP	S
Fe(1)-O(5)#1	0.6299	Fe(2)-O(23)	0.5473	Fe(3)-O(11)	0.4121	Fe(3)-N(5)	0.4679
Fe(1)-O(4)	0.6265	Fe(2)-O(30)	0.5385	Fe(3)-O(2W)	0.3719	Fe(4)-O(3W)	0.3476
Fe(1)-O(12)#1	0.4530	Fe(2)-O(2)	0.5020	Fe(3)-O(39)	0.3457	Fe(4)-O(4W)	0.3231
Fe(1)-O(2)#1	0.4143	Fe(2)-O(1W)	0.4591	Fe(3)-O(37)	0.3145	Fe(4)-O(36)	0.2940
Fe(1)-O(13)	0.4077	Fe(2)-O(12)#1	0.4469	Fe(3)-N(3)	0.3883	Fe(4)-O(38)	0.2800
Fe(1)-O(2)	0.4066	Fe(2)-O(13)#1	0.4409	Fe(3)-N(4)	0.3841	Fe(4)-N(11)	0.3365
				Fe(3)-N(5)	0.3810	Fe(4)-N(10)	0.3338
BVS	2.9380		2.9348		2.5977		2.3828

Section 5 The Selected bonds lengths and angles

Table S6. Selected bonds lengths (\AA) and angles ($^\circ$) for compound **1**.

W(1)-O(16)	1.735(10)	W(14)-O(38)	1.817(10)
W(1)-O(59)	1.870(9)	W(14)-O(30)	2.022(9)
W(1)-O(22)	1.877(10)	W(14)-O(65)	2.027(10)
W(1)-O(1)	1.931(11)	W(14)-O(24)	2.363(9)
W(1)-O(28)	1.936(9)	W(15)-O(15)	1.825(9)
W(1)-O(54)	2.370(9)	W(15)-O(5)#1	1.841(10)
W(2)-O(45)	1.706(10)	W(15)-O(37)	1.851(10)
W(2)-O(7)	1.879(10)	W(15)-O(6)	2.028(9)
W(2)-O(28)	1.899(10)	W(15)-O(33)	2.113(10)
W(2)-O(52)	1.915(10)	W(15)-O(43)	2.269(9)
W(2)-O(12)	1.924(10)	W(16)-O(5)	1.826(10)
W(2)-O(54)	2.385(9)	W(16)-O(9)	1.841(9)
W(3)-O(50)	1.704(11)	W(16)-O(4)	1.845(10)
W(3)-O(56)	1.878(10)	W(16)-O(39)	2.024(9)
W(3)-O(34)	1.884(10)	W(16)-O(41)	2.115(9)
W(3)-O(57)	1.933(10)	W(16)-O(36)	2.303(9)
W(3)-O(32)	1.951(9)	W(17)-O(4)	1.818(10)
W(3)-O(14)	2.412(9)	W(17)-O(15)	1.840(9)
W(4)-O(48)	1.706(10)	W(17)-O(3)	1.844(9)
W(4)-O(42)	1.876(10)	W(17)-O(20)	1.999(9)
W(4)-O(25)	1.902(10)	W(17)-O(21)	2.094(10)
W(4)-O(29)	1.924(10)	W(17)-O(46)	2.311(9)
W(4)-O(7)	1.925(10)	W(18)-O(37)	1.802(10)
W(4)-O(49)	2.344(9)	W(18)-O(9)	1.813(9)
W(5)-O(31)	1.714(10)	W(18)-O(3)#1	1.823(10)
W(5)-O(17)	1.834(10)	W(18)-O(17)	2.009(9)
W(5)-O(52)	1.889(10)	W(18)-O(38)	2.092(10)
W(5)-O(27)	1.886(9)	W(18)-O(64)	2.290(9)
W(5)-O(18)	1.972(10)	Fe(4)-O(15)	1.825(9)
W(5)-O(64)	2.341(9)	Fe(4)-O(5)#1	1.841(10)
W(6)-O(51)	1.743(10)	Fe(4)-O(37)	1.851(10)
W(6)-O(10)	1.861(10)	Fe(4)-O(6)	2.028(9)
W(6)-O(1)	1.872(10)	Fe(4)-O(33)	2.113(10)
W(6)-O(57)	1.905(10)	Fe(4)-O(43)	2.269(9)
W(6)-O(29)	1.940(10)	Fe(5)-O(5)	1.826(10)
W(6)-O(49)	2.398(10)	Fe(5)-O(9)	1.841(9)
W(7)-O(13)	1.714(9)	Fe(5)-O(4)	1.845(10)
W(7)-O(39)	1.825(9)	Fe(5)-O(39)	2.024(9)

W(7)-O(8)	1.865(10)	Fe(5)-O(41)	2.115(9)
W(7)-O(59)	1.934(9)	Fe(5)-O(36)	2.303(9)
W(7)-O(11)	1.963(9)	Fe(6)-O(4)	1.818(10)
W(7)-O(36)	2.377(9)	Fe(6)-O(15)	1.840(9)
W(8)-O(44)	1.707(10)	Fe(6)-O(3)	1.844(9)
W(8)-O(20)	1.878(9)	Fe(6)-O(20)	1.999(9)
W(8)-O(8)	1.919(10)	Fe(6)-O(21)	2.094(10)
W(8)-O(10)	1.943(10)	Fe(6)-O(46)	2.311(9)
W(8)-O(34)	1.945(10)	Fe(7)-O(37)	1.802(10)
W(8)-O(46)	2.390(9)	Fe(7)-O(9)	1.813(9)
W(9)-O(47)	1.722(10)	Fe(7)-O(3)#1	1.823(10)
W(9)-O(30)	1.868(10)	Fe(7)-O(17)	2.009(9)
W(9)-O(18)	1.875(10)	Fe(7)-O(38)	2.092(10)
W(9)-O(12)	1.906(10)	Fe(7)-O(64)	2.290(9)
W(9)-O(23)	1.940(10)	P(1)-O(54)	1.527(10)
W(9)-O(24)	2.397(8)	P(1)-O(36)	1.536(9)
W(10)-O(35)	1.719(11)	P(1)-O(64)	1.543(9)
W(10)-O(62)	1.871(9)	P(1)-O(24)	1.573(10)
W(10)-O(26)	1.884(10)	P(2)-O(49)	1.517(10)
W(10)-O(32)	1.918(9)	P(2)-O(46)	1.516(10)
W(10)-O(25)	1.944(10)	P(2)-O(43)	1.552(10)
W(10)-O(14)	2.405(10)	P(2)-O(14)	1.559(10)
W(11)-O(40)	1.724(10)	Fe(1)-O(61)	2.166(11)
W(11)-O(6)	1.847(9)	Fe(1)-O(2)	2.195(12)
W(11)-O(42)	1.908(10)	Fe(1)-N(10)	2.192(14)
W(11)-O(27)	1.937(10)	Fe(1)-O(1W)	2.200(13)
W(11)-O(26)	1.957(10)	Fe(1)-N(11)	2.204(13)
W(11)-O(43)	2.363(9)	Fe(1)-N(12)	2.213(13)
W(12)-O(19)	1.713(11)	Fe(1)-O(2W)	2.216(12)
W(12)-O(65)	1.846(10)	Fe(2)-O(31)	2.083(10)
W(12)-O(11)	1.874(9)	Fe(2)-O(3W)	2.095(13)
W(12)-O(23)	1.954(9)	Fe(2)-O(66)	2.119(11)
W(12)-O(22)	1.958(10)	Fe(2)-N(4)	2.176(14)
W(12)-O(24)	2.413(9)	Fe(2)-N(3)	2.210(15)
W(13)-O(60)	1.731(10)	Fe(2)-N(5)	2.223(14)
W(13)-O(21)	1.764(10)	Fe(2)-O(63)	2.231(11)
W(13)-O(33)	1.814(9)	Fe(3)-O(4W)	2.032(12)
W(13)-O(56)	2.006(10)	Fe(3)-O(60)	2.078(10)
W(13)-O(62)	2.014(10)	Fe(3)-O(58)#1	2.087(11)
W(13)-O(14)	2.350(9)	Fe(3)-O(5W)	2.133(12)
W(14)-O(58)	1.730(11)	Fe(3)-O(7W)	2.199(13)
W(14)-O(41)	1.790(9)	Fe(3)-O(6W)	2.239(12)
O(15)-Fe(4)-O(5)#1	103.9(4)	O(61)-Fe(1)-O(2)	75.6(4)

O(15)-Fe(4)-O(37)	95.5(4)	O(61)-Fe(1)-N(10)	71.2(5)
O(5)#1-Fe(4)-O(37)	99.6(4)	O(2)-Fe(1)-N(10)	146.7(5)
O(15)-Fe(4)-O(6)	159.0(4)	O(61)-Fe(1)-O(1W)	86.0(5)
O(5)#1-Fe(4)-O(6)	95.0(4)	O(2)-Fe(1)-O(1W)	90.8(5)
O(37)-Fe(4)-O(6)	90.1(4)	N(10)-Fe(1)-O(1W)	88.8(5)
O(15)-Fe(4)-O(33)	85.9(4)	O(61)-Fe(1)-N(11)	141.5(4)
O(5)#1-Fe(4)-O(33)	89.7(4)	O(2)-Fe(1)-N(11)	142.9(5)
O(37)-Fe(4)-O(33)	169.9(4)	N(10)-Fe(1)-N(11)	70.4(5)
O(6)-Fe(4)-O(33)	85.1(4)	O(1W)-Fe(1)-N(11)	91.5(5)
O(15)-Fe(4)-O(43)	85.6(4)	O(61)-Fe(1)-N(12)	147.9(5)
O(5)#1-Fe(4)-O(43)	167.2(4)	O(2)-Fe(1)-N(12)	72.4(5)
O(37)-Fe(4)-O(43)	87.7(4)	N(10)-Fe(1)-N(12)	140.9(5)
O(6)-Fe(4)-O(43)	74.4(4)	O(1W)-Fe(1)-N(12)	91.7(5)
O(33)-Fe(4)-O(43)	82.4(3)	N(11)-Fe(1)-N(12)	70.5(5)
O(5)-Fe(5)-O(9)	99.7(4)	O(61)-Fe(1)-O(2W)	92.0(4)
O(5)-Fe(5)-O(4)	97.8(4)	O(2)-Fe(1)-O(2W)	89.2(4)
O(9)-Fe(5)-O(4)	97.1(4)	N(10)-Fe(1)-O(2W)	90.0(5)
O(5)-Fe(5)-O(39)	101.8(4)	O(1W)-Fe(1)-O(2W)	177.9(5)
O(9)-Fe(5)-O(39)	156.3(4)	N(11)-Fe(1)-O(2W)	89.8(5)
O(4)-Fe(5)-O(39)	89.8(4)	N(12)-Fe(1)-O(2W)	90.3(5)
O(5)-Fe(5)-O(41)	92.2(4)	O(31)-Fe(2)-O(3W)	171.6(5)
O(9)-Fe(5)-O(41)	86.2(4)	O(31)-Fe(2)-O(66)	86.6(4)
O(4)-Fe(5)-O(41)	168.7(4)	O(3W)-Fe(2)-O(66)	85.5(5)
O(39)-Fe(5)-O(41)	83.1(4)	O(31)-Fe(2)-N(4)	94.5(5)
O(5)-Fe(5)-O(36)	172.4(4)	O(3W)-Fe(2)-N(4)	93.4(5)
O(9)-Fe(5)-O(36)	83.8(4)	O(66)-Fe(2)-N(4)	140.4(5)
O(4)-Fe(5)-O(36)	88.3(4)	O(31)-Fe(2)-N(3)	86.6(5)
O(39)-Fe(5)-O(36)	73.7(3)	O(3W)-Fe(2)-N(3)	93.4(5)
O(41)-Fe(5)-O(36)	81.3(3)	O(66)-Fe(2)-N(3)	70.8(5)
O(4)-Fe(6)-O(15)	97.1(4)	N(4)-Fe(2)-N(3)	69.8(5)
O(4)-Fe(6)-O(3)	99.6(4)	O(31)-Fe(2)-N(5)	96.7(5)
O(15)-Fe(6)-O(3)	99.3(4)	O(3W)-Fe(2)-N(5)	88.8(5)
O(4)-Fe(6)-O(20)	90.1(4)	O(66)-Fe(2)-N(5)	149.3(5)
O(15)-Fe(6)-O(20)	157.1(4)	N(4)-Fe(2)-N(5)	69.9(5)
O(3)-Fe(6)-O(20)	100.8(4)	N(3)-Fe(2)-N(5)	139.8(5)
O(4)-Fe(6)-O(21)	168.3(4)	O(31)-Fe(2)-O(63)	88.1(4)
O(15)-Fe(6)-O(21)	86.0(4)	O(3W)-Fe(2)-O(63)	87.8(5)
O(3)-Fe(6)-O(21)	91.0(4)	O(66)-Fe(2)-O(63)	79.5(4)
O(20)-Fe(6)-O(21)	83.0(4)	N(4)-Fe(2)-O(63)	140.0(5)
O(4)-Fe(6)-O(46)	88.9(4)	N(3)-Fe(2)-O(63)	150.1(5)
O(15)-Fe(6)-O(46)	83.9(4)	N(5)-Fe(2)-O(63)	70.1(5)
O(3)-Fe(6)-O(46)	170.4(4)	O(4W)-Fe(3)-O(60)	175.2(5)
O(20)-Fe(6)-O(46)	74.5(3)	O(4W)-Fe(3)-O(58)#1	92.7(5)

O(21)-Fe(6)-O(46)	80.2(4)	O(60)-Fe(3)-O(58)#1	92.0(4)
O(37)-Fe(7)-O(9)	95.7(4)	O(4W)-Fe(3)-O(5W)	89.3(5)
O(37)-Fe(7)-O(3)#1	97.0(4)	O(60)-Fe(3)-O(5W)	89.2(4)
O(9)-Fe(7)-O(3)#1	104.1(4)	O(58)#1-Fe(3)-O(5W)	96.1(4)
O(37)-Fe(7)-O(17)	91.2(4)	O(4W)-Fe(3)-O(7W)	91.3(5)
O(9)-Fe(7)-O(17)	156.0(4)	O(60)-Fe(3)-O(7W)	84.1(4)
O(3)#1-Fe(7)-O(17)	97.8(4)	O(58)#1-Fe(3)-O(7W)	173.8(4)
O(37)-Fe(7)-O(38)	169.8(4)	O(5W)-Fe(3)-O(7W)	88.7(5)
O(9)-Fe(7)-O(38)	86.3(4)	O(4W)-Fe(3)-O(6W)	95.1(5)
O(3)#1-Fe(7)-O(38)	92.1(4)	O(60)-Fe(3)-O(6W)	86.0(4)
O(17)-Fe(7)-O(38)	83.2(4)	O(58)#1-Fe(3)-O(6W)	88.0(4)
O(37)-Fe(7)-O(64)	87.6(4)	O(5W)-Fe(3)-O(6W)	173.8(5)
O(9)-Fe(7)-O(64)	85.5(4)	O(7W)-Fe(3)-O(6W)	87.0(5)
O(3)#1-Fe(7)-O(64)	168.7(3)		

Symmetry transformations used to generate equivalent atoms: #1 -x+1,-y+3,-z+1; #2 -x+1,-y+2,-z+2; #3 x,y-1,z+1; #4 -x,-y+2,-z+2; #5 x,y+1,z-1

Table S7. Selected bonds lengths (\AA) and angles ($^\circ$) for compound 2.

W(1)-O(11)	1.729(10)	W(8)-O(31)	1.726(10)
W(1)-O(14)	1.899(9)	W(8)-O(4)	1.819(9)
W(1)-O(6)	1.923(9)	W(8)-O(8)	1.878(9)
W(1)-O(22)	1.924(10)	W(8)-O(17)	1.988(10)
W(1)-O(19)	1.941(9)	W(8)-O(21)	2.012(9)
W(1)-O(18)	2.240(9)	W(8)-O(3)	2.238(9)
W(2)-O(24)	1.730(9)	W(9)-O(35)	1.699(10)
W(2)-O(5)	1.836(9)	W(9)-O(30)	1.800(9)
W(2)-O(26)	1.902(10)	W(9)-O(26)	1.928(10)
W(2)-O(15)	1.980(10)	W(9)-O(25)	1.942(10)
W(2)-O(9)	1.994(10)	W(9)-O(14)	2.025(9)
W(2)-O(1)	2.211(9)	W(9)-O(18)	2.242(9)
W(3)-O(34)	1.709(10)	Mo(1)-O(3)	1.813(9)
W(3)-O(15)	1.901(10)	Mo(1)-O(18)	1.813(9)
W(3)-O(6)	1.916(9)	Mo(1)-O(1)	1.823(9)
W(3)-O(7)	1.921(9)	Mo(1)-O(2)	1.850(9)
W(3)-O(10)	1.926(9)	Fe(1)-O(5)#1	1.930(9)
W(3)-O(1)	2.282(9)	Fe(1)-O(4)	1.932(9)
W(4)-O(28)	1.709(10)	Fe(1)-O(12)#1	2.052(9)
W(4)-O(9)	1.911(9)	Fe(1)-O(2)#1	2.085(9)
W(4)-O(12)	1.919(9)	Fe(1)-O(13)	2.091(9)
W(4)-O(10)	1.948(9)	Fe(1)-O(2)	2.092(9)
W(4)-O(33)	1.948(9)	Fe(2)-O(23)	1.982(10)
W(4)-O(1)	2.237(9)	Fe(2)-O(30)	1.988(9)
W(5)-O(16)	1.708(10)	Fe(2)-O(2)	2.014(9)

W(5)-O(13)	1.898(9)	Fe(2)-O(1W)	2.047(10)
W(5)-O(21)	1.905(10)	Fe(2)-O(12)#1	2.057(9)
W(5)-O(33)	1.947(10)	Fe(2)-O(13)#1	2.062(9)
W(5)-O(20)	1.989(10)	Fe(3)-O(11)	2.087(10)
W(5)-O(3)	2.231(9)	Fe(3)-O(2W)	2.125(14)
W(6)-O(27)	1.707(10)	Fe(3)-O(39)	2.152(14)
W(6)-O(23)	1.804(10)	Fe(3)-O(37)	2.187(12)
W(6)-O(25)	1.918(9)	Fe(3)-N(3)	2.205(14)
W(6)-O(8)	1.947(9)	Fe(3)-N(4)	2.209(15)
W(6)-O(22)	2.028(10)	Fe(3)-N(5)	2.212(16)
W(6)-O(18)	2.249(9)	Fe(4)-O(3W)	2.114(13)
W(7)-O(32)	1.726(10)	Fe(4)-O(4W)	2.185(14)
W(7)-O(17)	1.884(11)	Fe(4)-O(36)	2.190(12)
W(7)-O(19)	1.892(9)	Fe(4)-O(38)	2.203(12)
W(7)-O(7)	1.924(10)	Fe(4)-N(11)	2.221(14)
W(7)-O(20)	1.972(10)	Fe(4)-N(10)	2.230(14)
W(7)-O(3)	2.270(10)	Fe(4)-N(12)	2.231(13)
O(3)-Mo(1)-O(18)	108.4(4)	O(11)-Fe(3)-O(37)	90.1(4)
O(3)-Mo(1)-O(1)	107.6(4)	O(2W)-Fe(3)-O(37)	87.9(5)
O(18)-Mo(1)-O(1)	107.3(4)	O(39)-Fe(3)-O(37)	78.8(5)
O(3)-Mo(1)-O(2)	111.8(4)	O(11)-Fe(3)-N(3)	94.7(4)
O(18)-Mo(1)-O(2)	110.8(4)	O(2W)-Fe(3)-N(3)	86.2(6)
O(1)-Mo(1)-O(2)	110.7(4)	O(39)-Fe(3)-N(3)	149.2(5)
O(5)#1-Fe(1)-O(4)	96.4(4)	O(37)-Fe(3)-N(3)	71.1(5)
O(5)#1-Fe(1)-O(12)#1	94.4(4)	O(11)-Fe(3)-N(4)	89.0(4)
O(4)-Fe(1)-O(12)#1	95.5(4)	O(2W)-Fe(3)-N(4)	93.6(6)
O(5)#1-Fe(1)-O(2)#1	94.6(4)	O(39)-Fe(3)-N(4)	140.8(6)
O(4)-Fe(1)-O(2)#1	166.5(4)	O(37)-Fe(3)-N(4)	140.4(5)
O(12)#1-Fe(1)-O(2)#1	91.5(4)	N(3)-Fe(3)-N(4)	69.5(5)
O(5)#1-Fe(1)-O(13)	93.7(4)	O(11)-Fe(3)-N(5)	85.0(5)
O(4)-Fe(1)-O(13)	92.2(4)	O(2W)-Fe(3)-N(5)	95.9(6)
O(12)#1-Fe(1)-O(13)	168.1(4)	O(39)-Fe(3)-N(5)	71.9(6)
O(2)#1-Fe(1)-O(13)	79.3(3)	O(37)-Fe(3)-N(5)	150.1(6)
O(5)#1-Fe(1)-O(2)	169.5(4)	N(3)-Fe(3)-N(5)	138.6(6)
O(4)-Fe(1)-O(2)	93.1(4)	N(4)-Fe(3)-N(5)	69.1(6)
O(12)#1-Fe(1)-O(2)	80.2(3)	O(3W)-Fe(4)-O(4W)	175.9(6)
O(2)#1-Fe(1)-O(2)	76.6(4)	O(3W)-Fe(4)-O(36)	91.4(6)
O(13)-Fe(1)-O(2)	90.4(3)	O(4W)-Fe(4)-O(36)	84.5(5)
O(23)-Fe(2)-O(30)	88.7(4)	O(3W)-Fe(4)-O(38)	87.7(6)
O(23)-Fe(2)-O(2)	91.7(4)	O(4W)-Fe(4)-O(38)	91.7(5)
O(30)-Fe(2)-O(2)	91.9(4)	O(36)-Fe(4)-O(38)	79.1(4)
O(23)-Fe(2)-O(1W)	89.2(4)	O(3W)-Fe(4)-N(11)	90.5(6)
O(30)-Fe(2)-O(1W)	89.8(4)	O(4W)-Fe(4)-N(11)	92.5(5)

O(2)-Fe(2)-O(1W)	178.1(4)	O(36)-Fe(4)-N(11)	140.6(5)
O(23)-Fe(2)-O(12)#1	92.2(4)	O(38)-Fe(4)-N(11)	140.3(5)
O(30)-Fe(2)-O(12)#1	173.8(4)	O(3W)-Fe(4)-N(10)	88.5(6)
O(2)-Fe(2)-O(12)#1	82.0(4)	O(4W)-Fe(4)-N(10)	89.9(5)
O(1W)-Fe(2)-O(12)#1	96.3(4)	O(36)-Fe(4)-N(10)	71.3(5)
O(23)-Fe(2)-O(13)#1	173.3(4)	O(38)-Fe(4)-N(10)	150.1(5)
O(30)-Fe(2)-O(13)#1	90.8(4)	N(11)-Fe(4)-N(10)	69.4(5)
O(2)-Fe(2)-O(13)#1	81.6(4)	O(3W)-Fe(4)-N(12)	91.0(6)
O(1W)-Fe(2)-O(13)#1	97.4(4)	O(4W)-Fe(4)-N(12)	92.7(5)
O(12)#1-Fe(2)-O(13)#1	87.6(4)	O(36)-Fe(4)-N(12)	150.6(5)
O(11)-Fe(3)-O(2W)	177.4(6)	O(38)-Fe(4)-N(12)	71.7(5)
O(11)-Fe(3)-O(39)	91.7(5)	N(11)-Fe(4)-N(12)	68.7(5)
O(2W)-Fe(3)-O(39)	86.3(6)	N(10)-Fe(4)-N(12)	138.1(5)

Symmetry transformations used to generate equivalent atoms: #1 -x+2,-y,-z

References:

- Contant R, Klemperer W G and Yaghi O. *Inorg Synth.*, 1990, **27**, 104.
- N. Laronze, J. Marrot and G. Hervé, *Chem. Commun.*, 2003, **18**, 2360.
- A. A. Abu-Hussen and W. Linert, *Spectrochim. Acta, Part A*, 2009, **74**, 214.
- (a) X. M. Luo, N. F. Li, Z. B. Hu, J. B. Cao, C. H. Cui, Q. F. Ling and Y. Xu. *Inorg. Chem.*, 2019, **58**, 2463; (b) J. Shi, Y. Xiong, M. J. Zhou, L. Chen and Y. Xu. *RSC Adv.*, 2017, **7**, 55427; (c) G. H. Hu, H. Miao, H. Mei, S. Zhou and Y. Xu. *Dalton Trans.*, 2016, **45**, 7947; (d) Y. Y. Dong, G. H. Hu, H. Miao, X. X. He, M. Fang and Y. Xu, *Inorg. Chem.*, 2016, **55**, 11621.
- (a) W. H. Guo, X. L. Tong and S. B. Liu, *Electrochim Acta*, 2015, **173**, 540; (b) Y. W. Liu, S. M. Liu, X. Y. Lai, J. Miao, D. F. He, N. Li, F. Luo, Z. Shi and S. X. Liu, *Adv. Funct. Mater.*, 2015, **25**, 4480; (c) P. W. Huo, M. J. Zhou, Y. F. Tang, X. L. Liu, C. C. Ma, L. B. Yu and Y. S. Yan, *J. Alloys Compd.*, 2016, **670**, 198; (d) J. J. Xie, Y. Zhang, Y. L. Han and C. L. Li, *ACS Nano*, 2016, **10**, 5304.
- (a) J. Arias-Pardilla, H. J. Salavagione, C. Barbero, E. Morallon and J. L. Vázquez, *Eur. Polym. J.*, 2006, **42**, 1521; (b) L. Xu, H. Zhang, E. Wang, D. G. Kurth and Z. Li, *J. Mater. Chem.*, 2002, **12**, 654.
- (a) X. Q. Lin, X. Z. Li, F. Li, Y. Y. Fang, M. Tian, X. C. An, Y. Fu, J. Jin and J. T. Ma, *J. Mater. Chem. A*, 2016, **4**, 6505; (b) L. Salvati Jr, L. E. Makovsky, J. M. Stencel, F. R. Brown and D. M. Hercules, *J. Phys. Chem.*, 1981, **85**, 3700.
- C. Pichon, A. Dolbecq, P. Mialane, J. Marrot, E. Rivière, M. Goral, E. Rivière, M. Goral, M. Zynek, T. McCormac, S. A. Borshch, E. Zueva and F. Sécheresse, *Chem. Eur. J.*, 2008, **14**, 3189.
- B. Z. Lin, L. W. He, B. H. Xu, X. L. Li, Z. Li and P. D. Liu. *Cryst. Growth Des.*, 2008, **9**, 273.

-
10. (a) J. Sha, J. Peng, Y. Lan, Z. M. Su, H. J. Pang, A. X. Tian, P. P. Zhang and M. Zhu. *Inorg. Chem.*, 2008, **47**, 5145; (b) H. Fu, Y. G. Li, Y. Lu, W. L. Chen, Q. Wu, J. X. Meng, X. L. Wang, Z.-M Zhang and E.-B. Wang. *Cryst. Growth Des.*, 2011, **11**, 458.
 11. (a) B. Godin, J. Vaissermann, P. Herson, L. Ruhlmann, M. Verdaguera and P. Gouzerh, *Chem. Commun.*, 2005, **45**, 5624; (b) B. Botar, Y. V. Geletii, P. Kögerler, D. G. Musaev, K. Morokuma, I. A. Weinstock and C. L. Hill. *J. Am. Chem. Soc.*, 2006, **128**, 11268; (c) L. H. Bi, U. L Kortz, S. Nellutla, A. C. Stowe, J. V Tol, N. S. Dalal, B. Keita, and L. Nadjo. *Inorg. Chem.*, 2005, **44**, 896.
 12. (a) W. Zhao, P. Palffy-Muhoray. *Appl. Phys. Lett.*, 1994, **65**, 673; (b) D. G. McLean, R. L. Sutherland, M. C. Brant, D. M. Brandelik, P. A. Fleitz and T. Pottenger. *Opt. Lett.*, 1993, **18**, 858; (c) M. Sheik-Bahae, A. A. Said, T. H. Wei, D. J. Hagan and E. W. Van Stryland. *IEEE journal of quantum electronics.*, 1990, **26**, 760.